



# The prediction of the structure of members of the homologous series of the higher rare earth oxides

Z.C. Kang, L. Eyring\*

*Department of Chemistry and Biochemistry, Arizona State University, Tempe AZ 85287-1604, USA*

## Abstract

The structural principle supported by the determination of the structures of the anion-deficient, fluorite-related, homologous series of higher rare earth oxides, is reviewed. The principle is applied to predict the structure of the  $\beta(2)$  phase, one of the members of the homologous series,  $R_nO_{2n-2m}$ . Addition of the rule that during reaction or phase transformation, oxygen or vacant oxygen sites move in close-packed layers, allows the steps in the transformation of  $\beta(2)$  to its homologue  $\beta(3)$  to be shown. This transformation has been observed at atomic-resolution in the electron microscope and is interpreted in terms of intermediate forms that appear as modulated distortion waves sweeping the specimen. © 1998 Elsevier Science S.A.

*Keywords:* Fluorite-type structure principles; Modelling phase transformations; Higher rare earth oxides; Oxygen-deficient oxides; Fluorite-related oxides

## 1. Introduction

By connecting cation coordination polyhedra such as tetrahedra and octahedra by, for example, corner-sharing, edge-sharing, or face-sharing, it has been possible to elucidate the structures and compositions of the transition metal oxides [1,2]. Using similar ideas to solve the structural and compositional principles of fluorite-related, anion-deficient homologous series phases including the rare earth oxides have failed.

These fluorite-related oxides have been used as catalysis, sensors, electrochromic materials, varistors, mixed ionic and electronic conductors. It is important to improve our understanding of these useful properties within the framework of solid-state chemistry. An excellent place to begin is to understand the principles on which compositions and structures are based. Recently, the structural and compositional principles that underlie the fluorite-related, anion-deficient rare earth higher binary oxides have been published [3,4]. Work has begun toward applying this understanding of the structures and compositions to the properties of these systems. Use of these principles, not only successfully provides models for the known structures, but enables prediction of the structures

of any homologous series phase, for which the composition and suitable electron diffraction patterns are available. Specifically, these principles can aid in understanding characteristics such as the thermodynamics of the systems including phase transitions, kinetics, hysteresis, surface activity, and chemical reactivity.

In this paper, the predicted structure of the  $\beta(2)$  phase in the higher oxides of the rare earths, a polymorph of the known structure of  $\beta(1)$ ,  $R_{24}O_{44}$ , will be presented utilizing suitable electron diffraction patterns. The diffraction patterns indicate that although the volume of the unit cell is the same as for  $\beta(1)$ , the projected unit cell in the  $[112]_F$  zone is a parallelogram rather than a rectangle. The structure of the  $\beta(3)$  phase is also predicted and the transition from  $\beta(2)$  to  $\beta(3)$ , which has been observed in the electron microscope, is modeled.

## 2. The compositional and structural principles

The fluorite structure can be visualized as three interpenetrating face-centred cubic sublattices with two oxygen sublattices shifted  $\pm 1/4 [111]_F$  along one diagonal of the cation sublattice. In this description, the two oxygen sublattices are independent and have equal importance for forming the fluorite-related structures. The structure can also be viewed as eight tetrahedra with cations at the corners and the oxygen anions at the centres. Two types of

\*Corresponding author. Tel.: +1 602 9652747; e-mail: leyring@asu.edu

tetrahedra are distinguishable. Each of them forms a slab of edge-sharing tetrahedra. Edge-sharing superposition of the two slabs creates the fluorite structure.

The higher oxides of the rare earths are anion-deficient fluorite-related structures. It is assumed that the two sublattices of oxygens, or the eight oxygens in a fluorite unit cell, have an equal probability to become vacant. We distinguish three types of fluorite-type modules: (1) one with no oxygen vacancy (designated F, fig.); (2) one with one oxygen vacancy, two vacancies are distinguished: the vacancy is located in the top layer of tetrahedra sharing edges (denoted as  $U^i$ , with  $i=1,2,3,4$ , as indicated in Fig. 1b), or the vacancy belongs to the tetrahedra in the bottom

half of the unit cell (denoted as  $D_i$ , and there are also four of these as shown as Fig. 1.c); and (3) one with two oxygen vacancies (denoted as  $W_j^i$ , with  $i$  and  $j=1$  and 3, 2 and 4, 3 and 1, and 4 and 2, respectively, representing the upper and lower halves of the fluorite unit cell, see Fig. 1d). The number 1, 2, 3, 4 indicates the order of the tetrahedra in a fluorite module. The F module has a composition  $R_4O_8$ , the U or D module is  $R_4O_7$  and the W module is  $R_4O_6$ . The composition of any group of modules is simply the sum of their individual compositions.

The new compositional and structural principles [3] are based on two experimental determinations: (a) the compositions of each member of the homologous series is

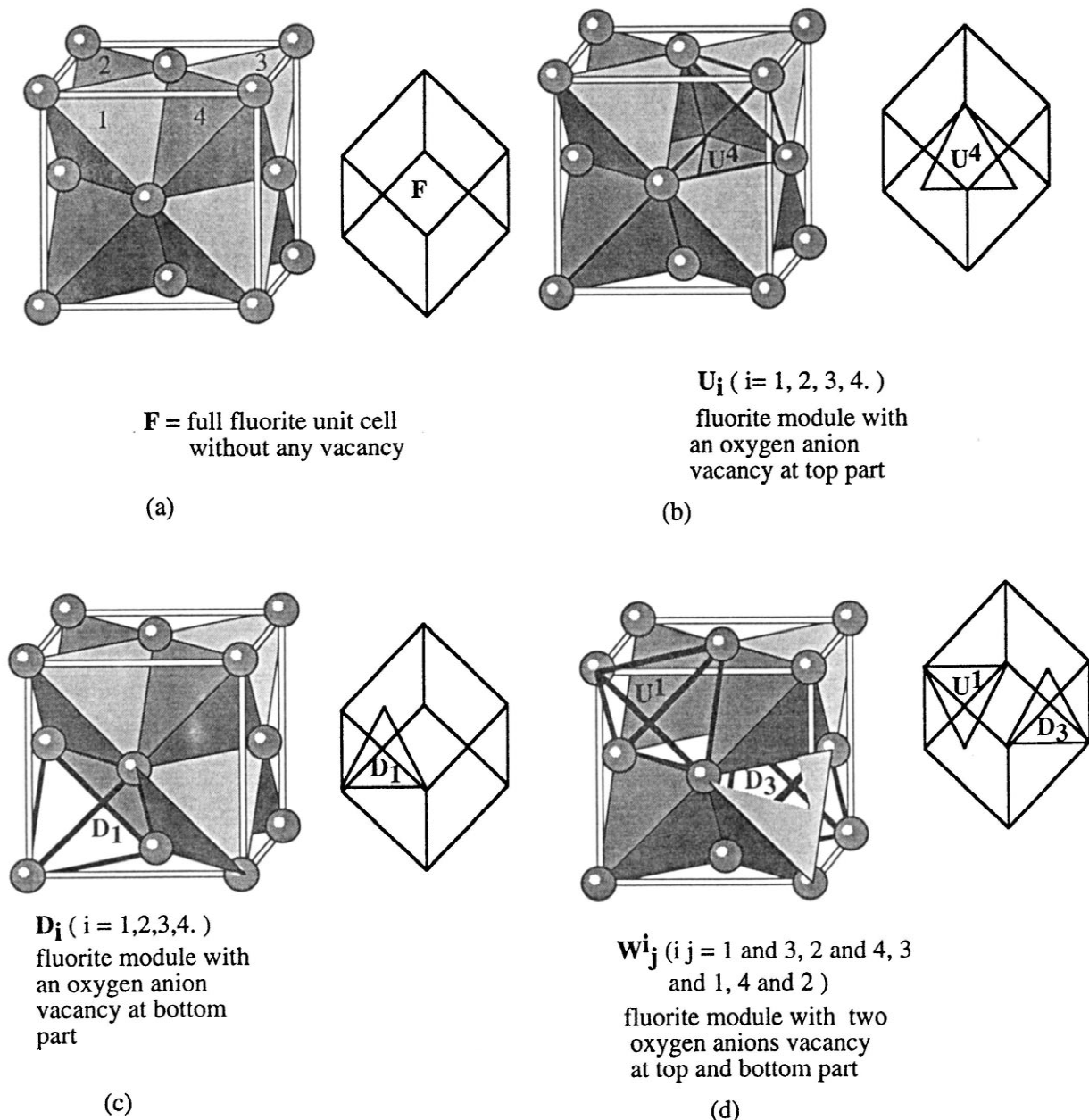


Fig. 1. The three varieties of fluorite-type modules: F,  $U^i$ ,  $D_j$ , and  $W_j^i$  and their projection along  $[112]_F$ .

determined analytically, usually gravimetrically, (b) the electron diffraction pattern is obtained from selected area or electron microdiffraction. It is possible, therefore, to obtain this necessary information from a small-sized crystal.

The compositional and the structural principles are as follows:

(1) Any homologous series phase of rare earth higher oxides is modeled by using the three varieties of fluorite modules (one without any oxygen vacancy, one with one oxygen vacancy, one with two oxygen vacancies) in which the basic fluorite unit cell is preserved, they suffer slight distortions in the real structure.

(2) The composition of any member of the homologous series,  $R_nO_x$ , is  $n_1R_4O_8 + n_2R_4O_7 + n_3R_4O_6$  and  $n = n_1 + n_2 + n_3$  ( $n_1$  is the number of F modules,  $n_2$  is the number of U and D modules,  $n_3$  is the number of W modules) which includes all the assembled modules. As postulated before the eight oxygens in a fluorite unit cell have an equal possibility to be vacant, Therefore any homologous series phase must have an integral number of the eight oxygen vacancies. However, the number of modules required to assemble the phase is not necessarily eight or a multiple of the eight. For example, for  $RO_{1.714}$  or  $R_7O_{12}$ , the number are  $n_1=0$ ,  $n_2=6$ , and  $n_3=1$  or  $n=7$ . The composition would be  $6 \times 4 + 1 \times 4 = 28$  for R ions;  $6 \times 7 + 1 \times 6 = 48$  for oxygen ions, this gives  $R_{28}O_{48}$  or  $RO_{1.714}$  or  $R_7O_{12}$ . There are, therefore, seven fluorite-type modules containing eight oxygen vacancies required to build the model of the iota phase. This leads to a generic formula for all possible members of the homologous series of rare earth higher oxides,  $R_{4n}O_{8n-8m}$  or  $R_nO_{2n-2m}$ , where  $n$  is the total number of modules required for assembling the phase,  $m$  is the integral multiple of the eight possibilities to remove an oxygen ion from a module. The deduced formula is also the number of atoms in the crystallographic unit cell of the phase.

(3) The ideal structure of any homologous series member is constructed by stacking the modules determined by its composition. The stacking sequences should have the configuration of lowest energy. This set of  $n$  modules should be extended one-to-one continuously to build the two and three dimensional structure of the phase. Because the eight oxygen sites have an equal possibility of being vacant, the U and D modules will be present in equal numbers. The unit cell deduced from the electron diffraction pattern is the guide for the modelling process.

(4) Oxygen or oxygen vacancies can migrate only within the close-packed layers. This will keep the two oxygen sublattices equal.

These principles have been tested by reproducing the ideal structures of the five series members that have been refined [3]. Furthermore, with respect to phase transformations they are consistent with the experimental thermodynamic data.

### 3. The predicted structure of the terbium $\beta(2)$ oxide

Based on the compositional and the structural principles, the modular content of the  $\beta(2)$  phase is the same as for  $\beta(1)$ ,  $n=24$ ,  $m=2$ ,  $R_nO_{2n-2m}$ . This requires 8F8U8D modules to model the structure of the  $\beta(2)$  phase. The electron diffraction pattern in the  $[112]_F$  zone shows the projected unit cell of this phase in this orientation. The diffraction pattern is used as a guide to sequencing the modules to predict the structure as shown in Fig. 2. In the first layer of fluorite-type modules (Fig. 2a) the  $D_1$ ,  $D_2$  and  $U^2$ ,  $U^3$  and, of course, F form oxygen-vacancy-pair configurations as they appear in this direction. However, it actually contains the pair ( $U^3$ ,  $D_1$ ) and single vacancies ( $D_2$ ,  $U^2$ ). In the second layer of fluorite-type modules (Fig. 2b) the  $D_3$ ,  $D_4$  and  $U^1$ ,  $U^4$  (of course F) form the same configuration as in the upper slab. Along the  $[112]_F$  direction, it appears that only vacancy pairs exist in the projected plane. The projected unit cell has the same volume as  $\beta(1)$ , but  $\beta(2)$  projects as a parallelogram (Fig. 2c). In three dimensions, as illustrated in Fig. 2d, the unit cell is seen to consist of a pair of oxygen vacancies at the origin and a pair inside the unit cell. The separated single oxygen vacancies in the first and second slab now connect through a metal ion to form a pair in the unit cell. The compositional and the structural principles are faithfully followed, and within the two layers all eight possible vacant positions occur in equal number. The atom positions, without the cation and anion distortions of the real structure, can be calculated based on this model. But the distortions can be approximated by reference of the refined structure of  $\beta(1)$  [5].

### 4. The phase transition from $\beta(2)$ to $\beta(3)$

The transition from  $\beta(2)$  to  $\beta(3)$  in the  $TbO_x-O_2$  system has been observed in the electron microscope at high-resolution [6]. The study revealed that the  $\beta(2)$  phase (the standard image of which is shown as Fig. 3a) was observed first. It was transformed to the  $\beta(3)$  phase (Fig. 3b shows the standard image) accompanied by sweeping modulation waves. An intermediate stage in the transformation is shown as Fig. 3d, in which a trace of the  $\beta(2)$  phase is present as a line of white dots. The distance between the white dots is the value related to the  $c$ -axis of the unit cell of  $\beta(3)$  phase. In the lower right-hand corner of the image, near a small insertion of the  $\beta(2)$  phase, the image is fading to the normal intensities of white dots representative of the fluorite sublattice. Modulation waves with different intervals exist. In some regions, it is close to the interval of the  $b$ -axis of  $\beta(3)$ . The modulation contrast in the  $\langle 110 \rangle_F$  orientation demonstrates the displacements of oxygen vacancies and nearby cations. The calculated image of the  $\beta(1)$  phase in the  $\langle 110 \rangle_F$  orientation is shown in Fig. 3c. It

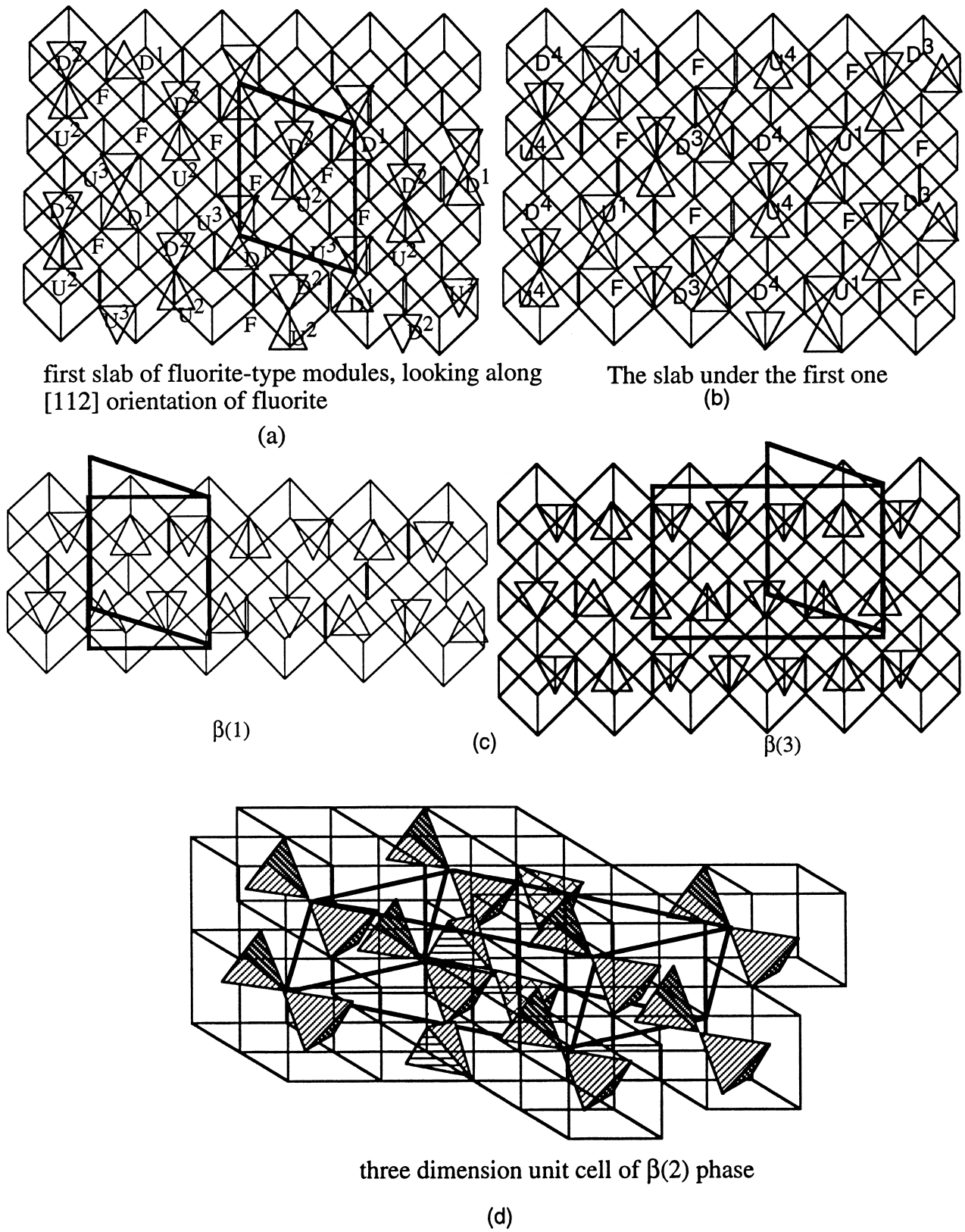


Fig. 2. The predicted structure of the  $\beta(2)$  phase: (a) the first slab of the modules projected along  $[112]_F$ , (b) the second slab of the modules, (c) the predicted structure of the  $\beta(1)$  and  $\beta(3)$  phases and the relationship between the projected unit cells of  $\beta(2)$ ,  $\beta(1)$ , and  $\beta(3)$  in  $[112]_F$  orientation, (d) the three dimensional unit cell of the  $\beta(2)$  phase.

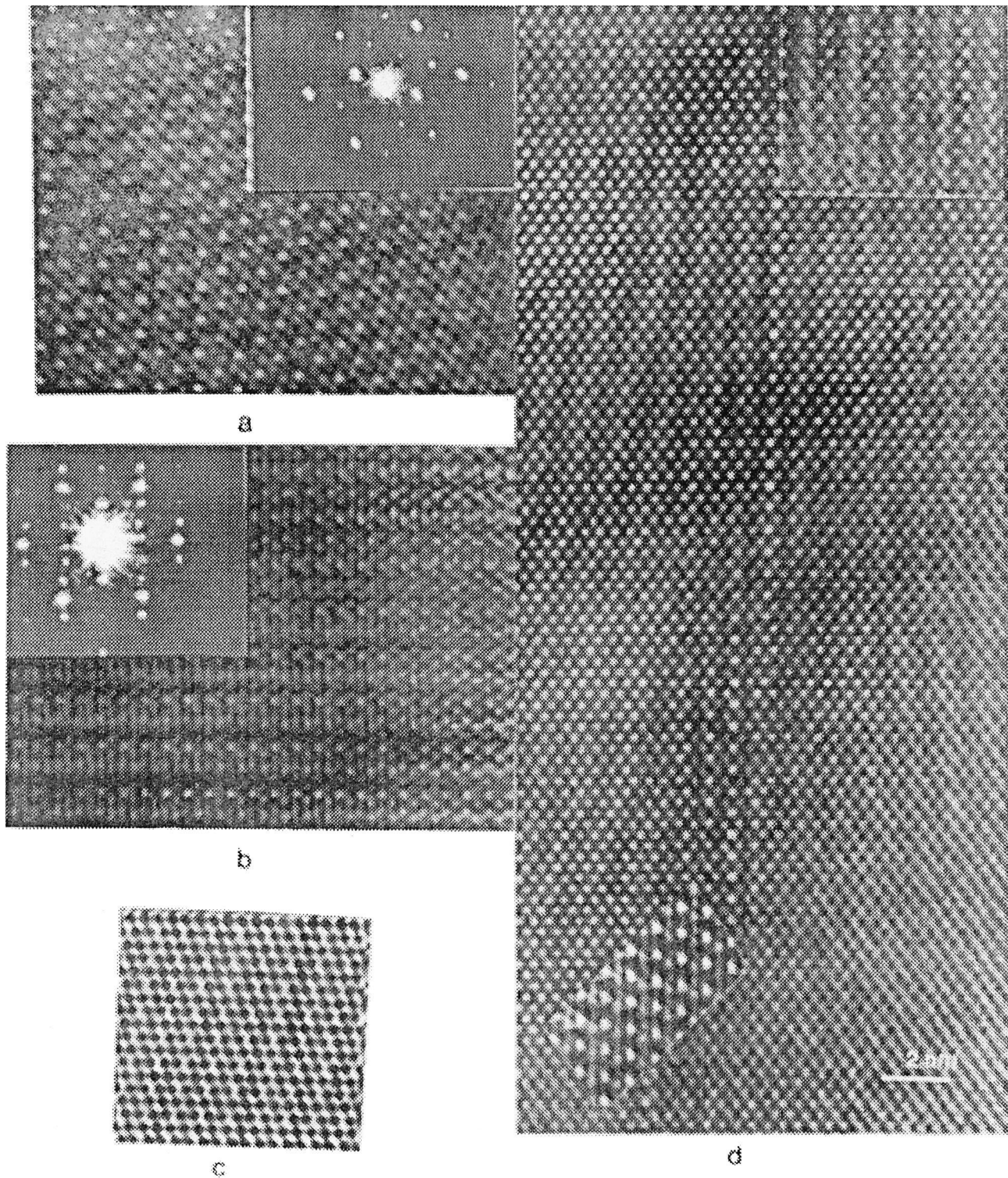


Fig. 3. The experimental high-resolution electron micrographs of (a)  $\beta(2)$  and (b)  $\beta(3)$ , (c) the calculated high-resolution image of the  $\beta(1)$  phase in the  $[110]_F$  zone, (d) an intermediate stage in the transformation from  $\beta(2)$  to  $\beta(3)$ .

also clearly shows the modulation contrast due to the oxygen vacancies and the cation distortion. This experimental event shows that the phase transition from  $\beta(2)$  to  $\beta(3)$  can be realized by oxygen or oxygen vacancy migration.

If the oxygen or oxygen vacancies migrate only within the close-packed layers (which are the  $\{1\ 1\ 1\}$  planes), and the compositional and structural principles are always obeyed, one can model a possible sequence of intermediate steps in the transformation from  $\beta(2)$  to  $\beta(3)$  as shown in

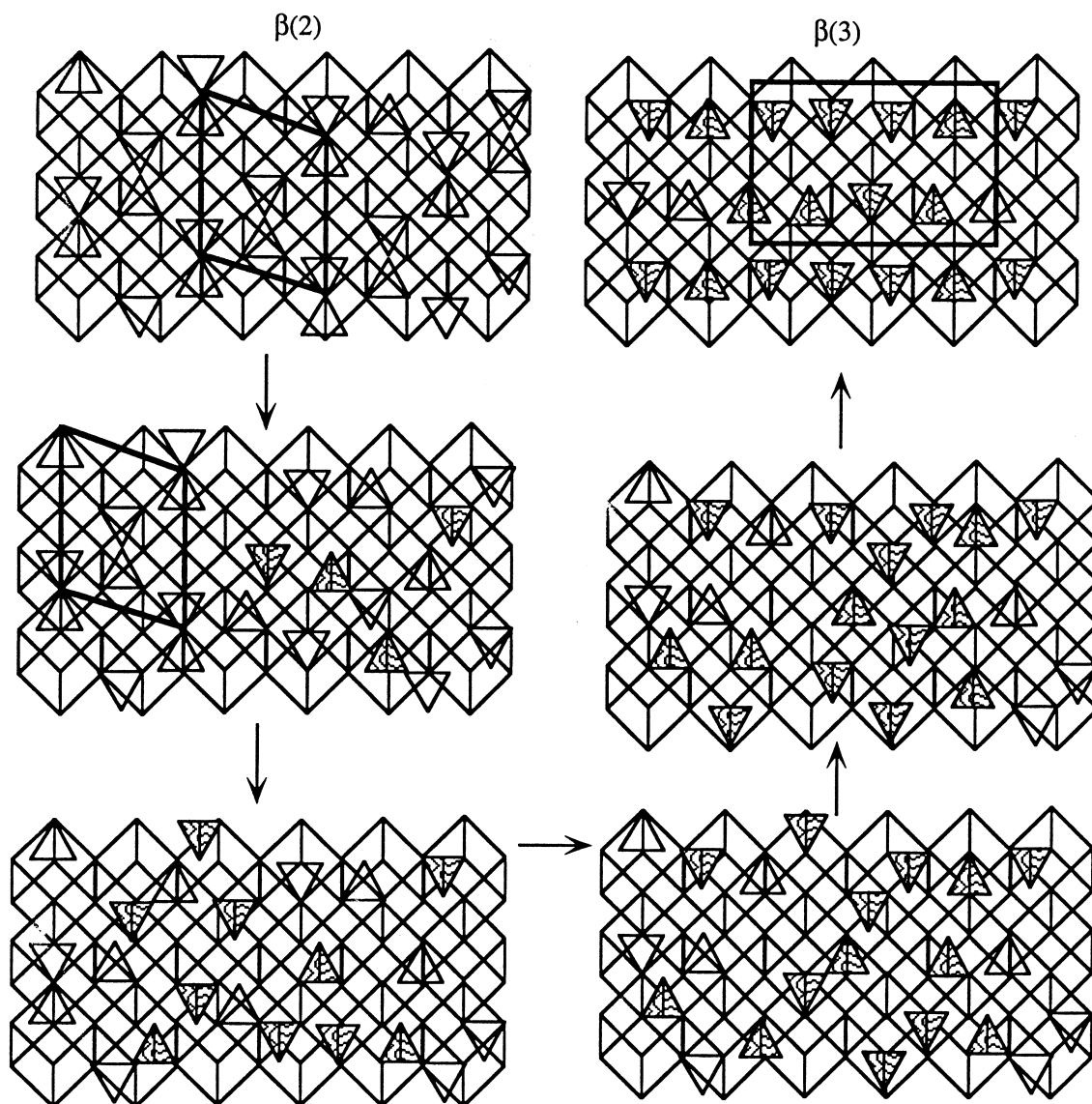


Fig. 4. A model of expected steps in the phase transformation between  $\beta(2)$  and  $\beta(3)$ .

Fig. 4. One must be aware that this is not an atomic-level mechanism for the phase transition, but it is a possible way for the transformation of  $\beta(2)$  to  $\beta(3)$  to occur. If these caveats are accepted, oxygen (or oxygen vacancy) migration on the closed packing layers is the primary process by which the transition can be brought about no matter whether or not a composition change occurs.

## 5. Conclusion

Using the compositional and structural principles for the fluorite-related, anion-deficient homologous series of rare earth oxides the structure of the  $\beta(2)$  phase ( $n=24$ ,  $m=2$ ) has been predicted and some steps in the phase transition from  $\beta(2)$  to  $\beta(3)$  have been modeled based on the

supposition that the oxygen (or vacancy) migration occurs only within close-packed layers. HREM observation of the actual transformation has been interpreted in terms of the modeled structures.

## Acknowledgements

We are grateful to Arizona State University for a grant that supported one of us, (Z.C. Kang).

## References

- [1] A.F. Wells, *Structural Inorganic Chemistry*, 5th ed., Clarendon, Oxford, 1984.

- [2] B.G. Hyde, S. Andersson, *Inorganic Crystal Structures*, J. Wiley and Sons, New York, 1989.
- [3] Z.C. Kang, L. Eyring, *Aust. J. Chem.* 49 (1977) 981.
- [4] Z.C. Kang, L. Eyring, *J. Alloys Comp.* 249 (1997) 206.
- [5] J. Zhang, R.B. Von Dreele, L. Eyring, *J. Solid-state Chem.* 122 (1996) 53.
- [6] Z.C. Kang, C. Boulesteix, L. Eyring, *J. Solid-state Chem.* 81 (1989) 96.